 doi:10.20944/preprints202107.0492.v1

Rochelle salt based ferroelectric and piezoelectric composite produced with simple additive manufacturing techniques

Etienne Lemaire[1], Damien Thuau[2], Jean-Baptiste De Vaulx[1], Nicolas Vaissiere[1] and Atilla Atli[1]

[1]Université de Lyon, ECAM Lyon, LabECAM, F-69005 Lyon, France.
[2]Université de Bordeaux, ENSCBP, F-33607 Pessac, France.

E-mail : etienne.lemaire@ecam.fr

Abstract

One century ago, ferroelectricity and then piezoelectricity were discovered using Rochelle salt crystals. Today, modern societies are invited to switch towards a resilient and circular economy model. In this context, this work proposes a method to manufacture piezoelectric devices made from agro-resources such as tartric acid and polylactide significantly reducing the energy budget without requiring any sophisticated equipement. These piezoelectric devices are manufactured by liquid phase epitaxy grown Rochelle salt (RS) crystals into a 3D printed poly(Lactic acid) (PLA) matrix being the artificial squared meshes which mimic the natural wood anatomy. This composite material can easily be produced in any fablab with renewable materials and at low processsing temperatures, reducing then the total energy consumed. Manufactured biodegradable samples are fully recyclable and have good piezoelectric properties without any pooling step. The measured piezoelectric coefficients of manufactured samples are higher than many piezoelectric polymers such as PVDF-TrFE.

Keywords: 3D printing, epitaxy, ferroelectric, piezoelectric salt, ecofriendly, composite

---

1. Introduction

The discovery of the piezoelectric effect is now more than one century old. Piezoelectricity consists in converting mechanical energy into electrical energy *i.e.* direct piezoelectric effect when a stress is applied on the sample. On the other hand, electrical to mechanical conversion happens when the voltage is applied on the sample *i.e.* the reverse piezoelectric effect. Since then, a large number of natural[1,2] and synthetic materials[3,4] have been reported with heterogeneous piezoelectric properties for numerous applications: sensors, motors, actuators, and energy harvesters[5,6]. The major piezoelectric materials are inorganic ferroelectric perovskites such as Lead Zirconate Titanate (PZT) and Barium Titanate (BTO). Environmental incompatibilities (toxicity, high sintering temperatures, etc.), as well as complex manufacturing procedures, have not prevented the widespread use of these ceramic materials, which are still extensively employed in industry. They are still used due to their very high ferroelectric and piezoelectric coefficients. As a matter of fact, researchers have intended to continuously optimized these features over the years e.g. by modifying their composition[7,8]. However, nowadays, piezoelectric organic ferroelectrics are attracted increasingly attention due to their lower manufacturing environmental impact. Among them, single crystals of diisopropylammonium bromide (DIPAB)[9] and croconic acid[10] are shown remanent polarizations of hundreds of $mC.m^{-2}$. Piezoelectric constants d_{33} of nearly 110 $pC.N^{-1}$ in polyamide 11/$NaNbO_3$ nanowire composites[11] have been measured. A coefficient of 40 $pm.V^{-1}$ in thin layers of imidazolium perchlorate [12,13], or even more than -60 $pm.V^{-1}$ has been obtained in devices of polyvinylidene-fluoride-trifluoroethylene (PVDF – TrFE) [14,15] or other organic crystals or materials [16–18]. Even if new piezoelectric materials are continuously discovered, the traditional materials (PZT, BTO, quartz) are still used, integrated and studied[19], while the oldest ones are somewhat surprisingly abandoned. Amongst which, Potassium sodium tartrate tetrahydrate ($KNaC_4H_4O_6.4H_2O$), also known as Seignette or Rochelle salt (RS) is ferroelectric between - 18°C and 24.9°C (its two Curie temperatures)[20]. RS exhibits high piezoelectric and dielectric constants. RS has a monoclinic structure in the ferroelectric

Preprints (www.preprints.org) | NOT PEER-REVIEWED | Posted: 21 July 2021 doi:10.20944/preprints202107.0492.v1

phase and an orthorhombic structure in the paraelectric phase [21]. Rochelle salt is also soluble in water and non-toxic (RS: E337 food additive is an approved by the Food and Drug Administration). Its low cost and ease of synthesis are some of its additional assets. It exhibits piezoelectric coefficient that can be higher than 100 pm.V^{-1}[22]. Nevertheless, direct piezoelectric coefficients and coupling factors have not been recently reported by the insight of performant new apparatus. This lack of interest might be due to its deprecated performances regarding its temperature and stability issues. Thus, this material has been excluded from technological applications during the past century. Nevertheless, from an environmental perspective, RS has some advantages in terms of ease of production, process simplicity, biocompatibility and biodegradability, resource scarcity, and intrinsic piezoelectric coefficient compared to most of lead-based and lead-free piezoelectric elements. Additionally, some cooperatives still produce RS as a by-product of the wine industry and thus can be considered as a renewable agro-resource. Recently, we have shown the possibility to grow RS crystals into cellulose-based sheets[23] or into the naturally orientated capillaries of wood[24] to create eco-friendly piezoelectric transducers.

Here, an innovative perspective based on this green material is presented which consists in growing crystalline salt into a 3D printed biodegradable polymer matrix making its manufacturing feasible in any *fablab*. We have developed 3D printed fully biodegradable piezoelectric salt composites. After the additive manufacturing of the PLA matrix, liquid phase epitaxial growth of RS crystals is performed with controlled crystalline orientation. The 3D printed PLA matrix imitates the natural wood tubular structure which has been recently studied[24]. The biodegradable PLA matrix having some good mechanical properties reinforces the salt based composite by encapsulating the brittle RS crystals. The millimetric mesh size of 3D printed PLA matrix favours the growth of single crystals having the same crystal orientation and improves then the piezoelectric performance.

2. Results and discussion

Herein, a simple approach is initiated where disk shaped piezoelectric samples composed by a 3D printed PLA matrix and RS were manufactured by following the process described in the Experimental section (Fig. 1). The manufactured samples were characterized by using direct and converse piezoelectricity measurements associated to the impedance spectroscopy in order to illustrate the resonant device behavior and ferroelectricity.

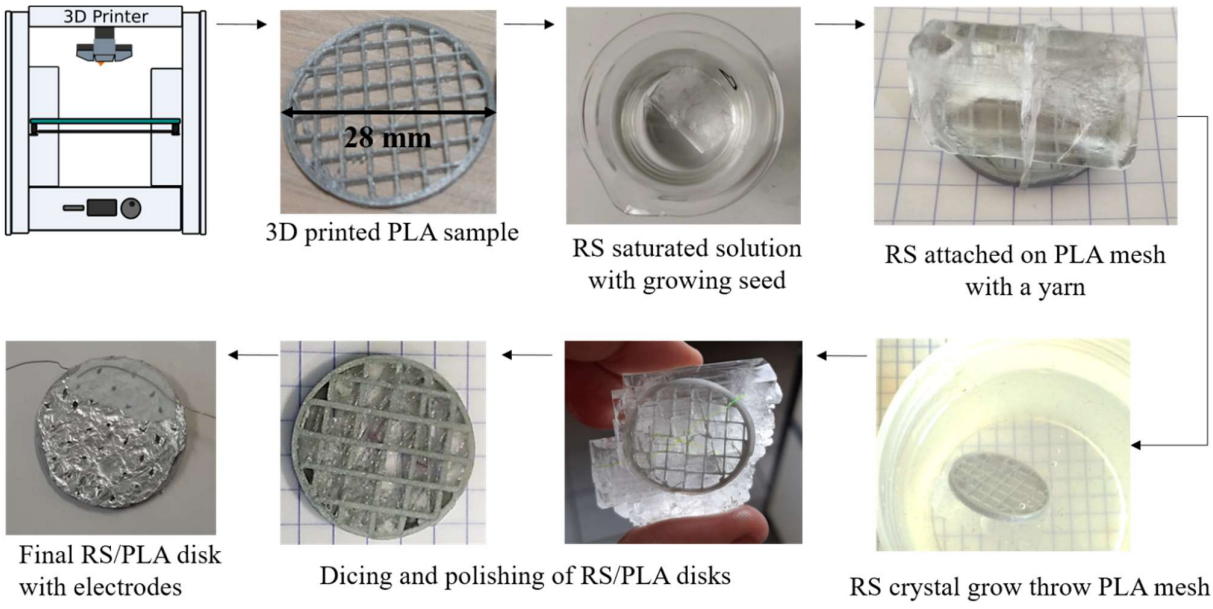

Figure 1. Manufacturing process flow of the piezoelectric samples.

Preprints (www.preprints.org) | NOT PEER-REVIEWED | Posted: 21 July 2021 doi:10.20944/preprints202107.0492.v1

2.1. Ferroelectricity

In order to measure the effective ferroelectric behavior of devices, the capacitance under polarization were measured (Fig.2). A square shaped (10 mm side and 1 mm thick) pure RS crystal and PLA/RS composite disk (28 mm of diameter and 1 mm thin) have been pooled from -40V to +40V (and from +40V to -40V in order to highlight hysteresis loop) and capacitance at 10kHz were mesured each 200 mV (ten times). The impedance of the RS is strongly dependent on the temperature up to 10% of impedance variation per degree [25]. A precise temperature control (+/- 0.1 ° C) was necessary in order to observe ferroelectric behavior whith minimized temperature effects. Thus, impedance variation with respect to polarization was varying in the same range (10% of impedance variation for the full scale of bias voltage available : 40V). Pure RS sample has capacitance variation from 65 to 85 pF during the polarization cycle (and impedance from 0.9 to 1.2 MΩ with bias voltage varying from -40V to +40V). PLA/RS disk has similar behavior with capacitance variation of 116 to 128 pF during the polarization cycle. These measurement were performed near 10°C and similar curves have been obtained up to 15°C. The typical hysteresis loop can be observed on capacitance measurement on both devices (Fig. 2). Therefore, the ferroelectric characterization of Rochelle salt established in 1947 [26] and after [27, 28] was only partially reproduced. The few experimental literrature sources on Rochelle salt ferroelectricity suggest that we could reinvestgate Rochelle salt ferroelectric specificities under several environmental conditions (temperature and humidity) with modern equipement and more sophisticated and dedicated experimental setup.

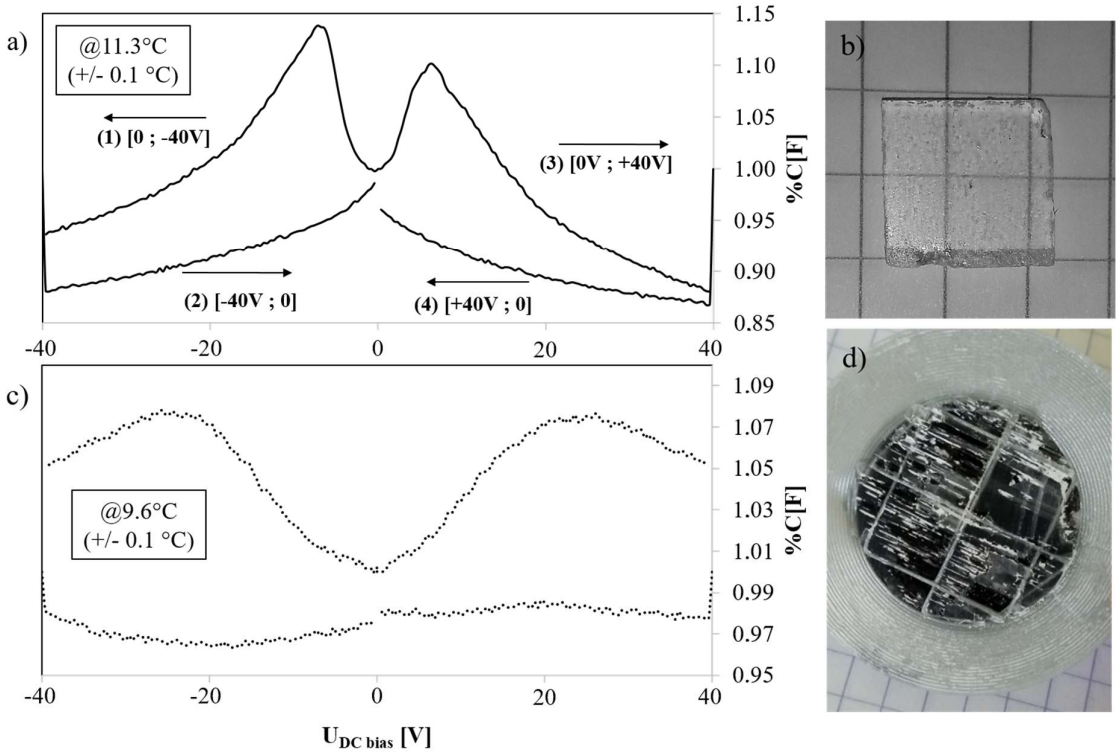

Figure 2. Normalized capacitance hysteresis loop measured on (a,b) thin RS square single crystal and (c,d) on RS/PLA thin sample, with bias voltage applied from -40 V to +40V.

2.2. Direct piezoelectricity

In order to measure the effective d_{33} coeficient a controlled force step was applied on the sample and the sample output current was recorded (Fig.3). Then the amount of charges was integrated in order to get the d [pC.N^{-1}] coefficient by using the known applied effective force. For a same applied force, most of the composite samples were responding with a higher electrical current than commercial PVDF-TrFE samples (MEAS piezoelectric film provided by TE Connectivity, dimensions: 41mm*16mm*40µm) loaded on 1MΩ.

Preprints (www.preprints.org) | NOT PEER-REVIEWED | Posted: 21 July 2021 doi:10.20944/preprints202107.0492.v1

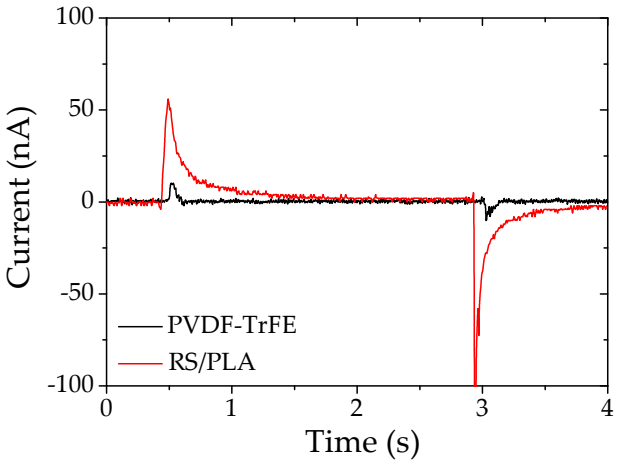

Figure 3. Harvested current respectively for one RS/PLA sample and the commercial PVDF-TrFE sample measured throw 1MΩ input impedance under a pressure step of 0 to 1 bar.

The d_{33} coefficients (Table 1) were calculated from electrical charges harvested under the same pressure step of 0 to 1 bar for manufactured PLA/RS composite samples for two different thicknesses and for a commercial PVDF-TrFE sample. The results show that RS/PLA samples have higher d_{33} coefficient under this pressure. The commercial PVDF-TrFE has a repeatable d_{33} of 21 pC.N^{-1}. The manufactured 2.5 mm and 1.5 mm thick RS/PLA samples have an average d_{33} of 39 pC.N^{-1} and 119 pC.N^{-1} respectively at the same ambient conditions. Therefore our manufactured composite thick disks have suprisingly high piezoelectric characteristics compared to commercial ultra-thin PVDF-TrFE. In our recent work where RS crystals have been grown in a natural wood matrix structure, an avarage value of 11. pC.N^{-1} for d_{33} has been found [24]. It is worth noting that some thin PLA/RS samples (thickness of 1.5 mm) have non negligeable residual stress due to the 3D printing process, resulting in a curved shape rather than a flat sample. A stronger electrical response is thus recorded in this case due to the fact that the mechanical deformation includes not only pure compression but also deflection of the disk. Then, the piezoelectricity in other directions is probably induced and other coefficients like d_{13} and d_{14} are probably solicited. Note that those coefficients could not be measured on our samples. The average coefficients are included into a large uncertainty interval for RS/PLA samples due to reproducibility of the manufacturing process. In fact, cristallisation around defects of 3D printed PLA matrices and residual stress issues led to samples with varying performances. Nevertheless these results are confirmed by converse piezoelectricty measurements. Injected PLA matrices with a clean surface state could enhance the reproducibility.

Table 1. Average values (μ), and their corresponding standard deviation (σ) of direct piezoelectric coefficients calculated from charges harvested under a pressure step of 0 to 1 bar, converse piezoelectric coefficients calculated from static displacement and applied voltage, resonant frequencies (f_r [Hz]), quality factors (Q), and coupling factors (k_p) extracted from impedance spectra. for two thicknesses (1.5 mm and 2.5 mm) of RS/PLA composite samples and for a commercial PVDF-TrFE sample.

		Direct d_{33} [pC.N^{-1}]	**Converse d_{33} [pm.V^{-1}]**	**f_r[Hz]**	**Q**	**k_p**
1.5 mm	μ	119	80	37 433	34	0.25
	σ	56	16	6226	13	0.04
2.5 mm	μ	55	32	49 132	83	0.16
	σ	19	14	3106	25	0.02
PVDF-TrFE	μ	22	*NA*	*NA*	*NA*	*NA*
	σ	1				

Preprints (www.preprints.org) | NOT PEER-REVIEWED | Posted: 21 July 2021 doi:10.20944/preprints202107.0492.v1

2.3. Converse piezoelectricity

AC signals have been applied to the manufactured RS/PLA composite samples and their displacements and electrical characteristics recorded with a laser vibrometer and impedance analyser. Both characterizations highlighted the same converse piezoelectric effect. For instance, the same sample measured with both techniques (Fig.4) shows the same principal resonant mode on conductance and out-of-plane displacement. The converse effective d_{33} [pm.V^{-1}] coefficient was calculated by measuring the static displacement of the sample using the second order approximation of spring-mass-damper system given by:

$$H_0 = 2\xi H(f_0) \quad (1)$$

with H_0 is the static displacement, ξ is the damping ratio and $H(f_0)$ is the maximum displacement at the Eigen frequency f_0. The static displacements were calculated for several applied voltages U, oscillating at f_0 and reported (Fig.5). The displacement was found to increase linearly with the applied voltage. The slope of this linear function leads to the experimental effective converse d_{33} coefficient. The comparison of converse piezoelectric coefficients calculated from static displacement and applied voltage, for two thicknesses of RS/PLA manufactured samples (Table 1) confirms the general trend measured for direct piezoelectric effect characterization. 2.5 mm thick fully biodegradable RS/PLA samples have an average d_{33} of 31 pm.V^{-1} and 1.5 mm thick RS/PLA samples have 80 pm.V^{-1}. Reminding that, under laser vibrometer, displacement is measured in the same direction of applied electric field (more consistent d_{33} measurement), the sample residual stress is mostly eliminated from the sample out-of-plane response (measured only in this direction). Therefore, the coefficient calculated from converse piezoelectricity for thin samples is lower compared to the average one measured under mechanical solicitation. Additionally, the coefficient from converse piezoelectricity for thick PLA/RS sample is closer to the one obtained in direct piezoelectricity. This should be due to the absence of residual stress in thicker samples.

Thicker samples have lower effective d_{33} coefficient than thinner ones. It is then important to clarify the thickness dependence of effective d_{33} coefficient. Theoretically, liquid phase epitaxy permit crystals growth in only one crystallographic direction which is the seed crystal direction (homogenous growth). Nevertheless, in our case, the crystallisation can also be initiated on the walls of PLA matrix due to the defects on its rough surface (heterogeneous growth). Thus, as the crystallisation progresses without facing the imperfect PLA matrix surface, the initial seed crystallisation direction is further conserved. The increased contact surface in thicker PLA matrices increases other potential nucleation points for RS crystal growth on PLA walls. This is then a competition between homogenous and heterogeneous crystal growth. Therefore, in thicker samples the RS crystals growth in the PLA channels are probably more randomly oriented than in thin ones, resulting in a deprecated effective d_{33}.

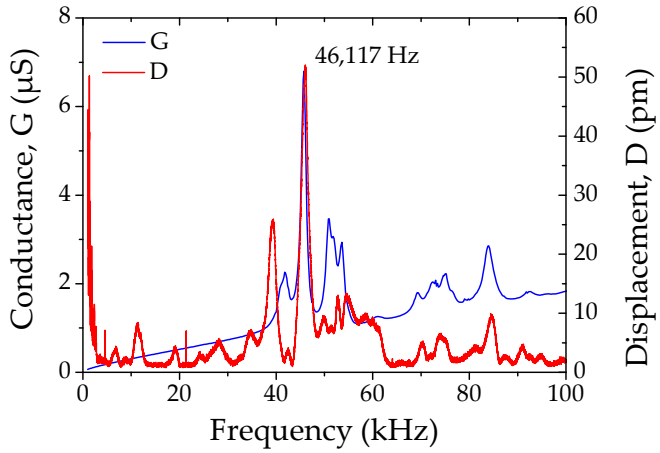

Figure 4. Conductance vs displacement spectra recorded on the same sample (2.5 mm thick) respectively using impedance spectrum (U=1V) and laser vibrometer (U=2V).

Preprints (www.preprints.org) | NOT PEER-REVIEWED | Posted: 21 July 2021 doi:10.20944/preprints202107.0492.v1

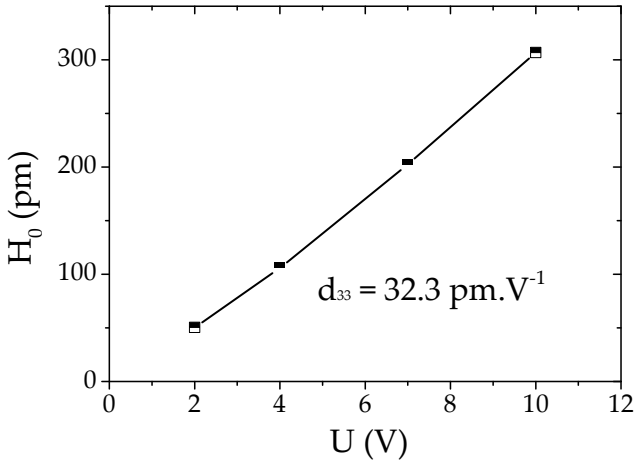

Figure 5. Static displacement (computed from vibrometer measurements) vs applied voltage measured on one RS/PLA 2.5 thick sample.

Then, impedance spectroscopy was used to characterize each manufactured RS/PLA composite sample. The conductance and susceptance spectra (Fig.6) allowed to identify the resonant behavior of the piezoelectric samples and define their resonance frequency (f_r), quality factor (Q) and coupling coefficient (k_p). The average values and standard deviation of those parameters (Table 1) are shown for the two geometries of manufactured disks. Thicker (2.5 mm) samples have higher resonance frequencies ($f_r \approx 49$ kHz) and quality factors ($Q \approx 80$) than thinner (1.5 mm) samples ($f_r \approx 38$ kHz and $Q \approx 37$). This is probably due to the increased stiffness of thicker RS/PLA samples compared to thinner ones. In terms of coupling factors, thinner disks have better coefficients ($k_p \approx 0.25$ for 1.5 mm and 0.15 for 2.5 mm). We can notice that Q factors obtained are the higher reported for RS with such simple and environmentally friendly technology.

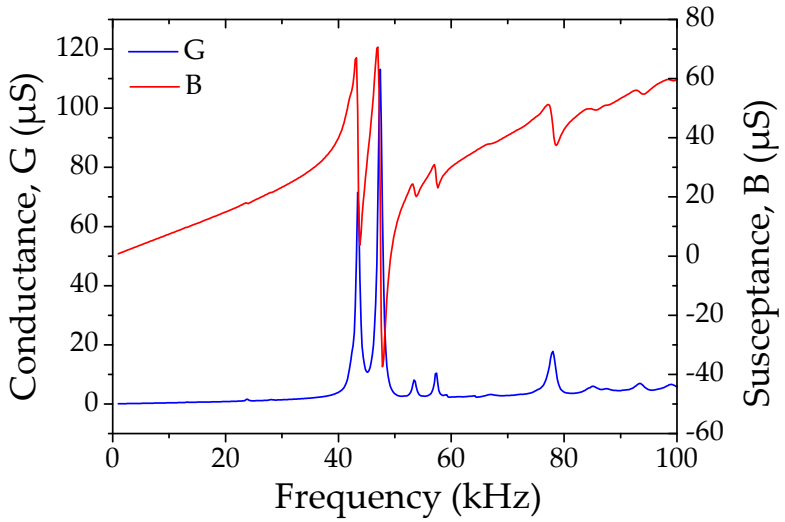

Figure 6. Conductance and susceptance spectra of 2.5 mm thick RS/PLA manufactured sample.

3. Conclusion

In this work, we demonstrated the ferroelectric and piezoelectric performance of ecofriendly PLA/RS composites obtained by using additive manufacturing techniques. The samples are made by growing the Rochelle salt crystals into a 3D printed biodegradable PLA matrix with millimetric meshes. A RS seed is attached to one side of the disk shaped PLA matrix and used for favouring the crystal orientation into the

Preprints (www.preprints.org) | NOT PEER-REVIEWED | Posted: 21 July 2021 doi:10.20944/preprints202107.0492.v1

matrix capillaries. Then, the direct and converse piezoelectric properties of RS/PLA composite samples were characterized. Additionally the ferroelectric behaviour has been illustrated below Curie point at 24.9°C. In terms of piezoelectric performance, we achieved an effective d_{33} of 30 pC.N^{-1} and 120 pC.N^{-1} on 2.5 mm and 1.5 mm thick PLA/RS composite samples, respectively. The transducers have a resonance frequency in the kilohertz range with quality factors ranging from 20 to 100. The d_{33} of manufactured samples is higher than most of commercial PVDF-TrFE films. We demonstrated that RS/PLA samples can easily be made at low cost in any *fablab* and with an eco-friendly approach. They have strong advantages in terms of cost, environmental impacts and energy budget, compared to most of lead-based and lead-free piezoelectric components. This is partially due to process simplicity and few (thermal) energy required. The performances of such 3D printed fully biodegradable piezoelectric composites could be of great interest for disposable harvester, sensor or actuator applications. In the future, circular manufacturing of such piezoelectric-salt based components could be further developed to produce some components limiting the material intensity and minimizing the environmental impacts. For the moment, this technology perfectly match actual pedagogical needs and application, illustrating advanced physical or technological concepts and applications with "low systemic environmental footprint" process in coherence with student requests. They recently asked academic institutions to switch urgently to contents and concrete experiments that could help to prepare themselves to climate change challenges. To start to achieve this request, "green" experimental matters and materials, could be used to highlight industrial (more polluting) equivalent technological concepts or elements. Authors think that the methods, materials and experiments presented in this work are in accordance with this eco-friendly academic transition, especially in the field of sensors and transducers development.

4. Experimental Section

PLA/RS sample manufacturing:

First PLA matrices have been printed using Ultimaker 3D printer (V1.1) and PLA filament also provided by the same company. In parallel, some RS crystal seeds were grown in order to get large single crystals at least 2 cm wide. The crystal growth was performed in an over saturated solution at room temperature (around 21°C) by mixing deionized water and RS powder provided by APC pure company (UK). Then a RS seed was attached to a disk shaped PLA matrix on one side and deep into the solution kept at 10°C in order to initiate the liquid phase crystal epitaxy through the PLA disk as shown in Fig.1. Once the PLA sample was completely embedded into the growing RS crystal (after 36 to 48 hours), it is removed from the solution. Then the samples were naturally dried and the exceeded RS from PLA matrix was removed by cutting the RS crystal close to both sides of disk and polished by sanding paper until the PLA matrix surfaces appear again. Finally, electrodes were placed on the sample: two aluminium disks (10 µm thin) were cut into a commercial aluminium foil and stick on both faces of the disk with Bare conductive ink (commercial name: "electric paint"). As mentioned previously, this manufacturing process is simple and feasible in any *fablab* without any sophisticated equipment. Both energy and financial budgets of such a process are low compared to standard piezoelectric ceramic or even organic samples in terms of costs and of complexity.

Experimental setup and characterization tools:

For each 3D printed fully biodegradable piezoelectric composite sample, we measured the impedance spectrum of the PLA/RS samples by using E4980A, Keysight impedance analyser. The displacement spectra were acquired by employing a MSA-500 laser vibrometer from Polytech. The direct piezoelectric effect was evaluated with a dedicated setup described in Fig.7. It consists of a pressure-controlled compressed air piston applying a controlled pressure to the sample, behind which a sensor indicating the applied force to the sample. The output piezoelectric signal is measured on a scope (TDS2014C, Tektronix) loaded on 1 MΩ or 10 MΩ. The calculation of electrical charges (Coulombs) is performed using a digital integration after noise reduction of the signal.

Preprints (www.preprints.org) | NOT PEER-REVIEWED | Posted: 21 July 2021 doi:10.20944/preprints202107.0492.v1

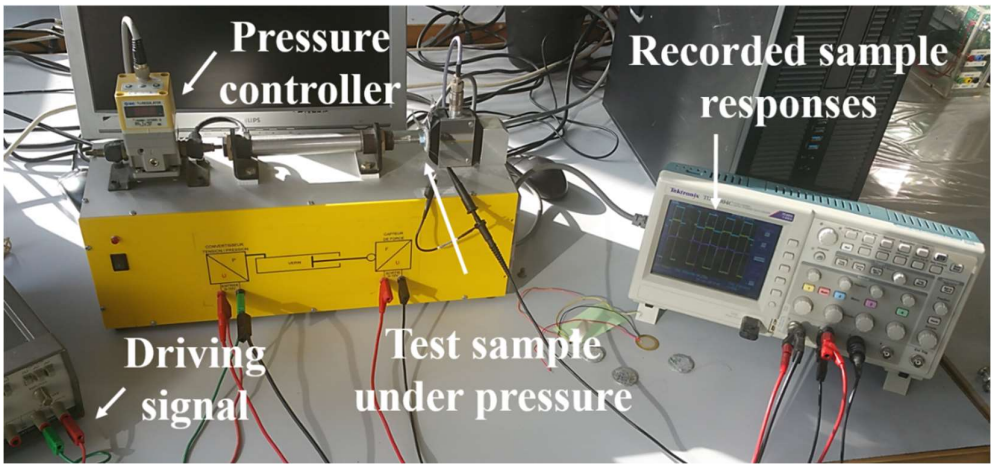

Figure 7. Dedicated direct piezoelectric coefficients measurement setup.

Acknowledgements

Authors would like to thank Christophe Jouve and Pierre Lourdin for their support on the "*PiezoSalt 3D*" internal project at ECAM Lyon. They let us some time to work on this unusual project and permits us to have students partially working on it.

References

[1] C. Brown , R. Kell, R. Taylor and L. Thomas , Piezoelectric Materials, A Review of Progress, *IRE Trans. Compon. Parts*, 1962, **9** , 193 —211 CrossRef .
[2] W. L. Bond A Mineral Survey for Piezo-Electric Materials, *Bell Syst. Tech. J.*, 1943, **22** , 145 —152 CrossRef.
[3] P. K. Panda Review: environmental friendly lead-free piezoelectric materials, *J. Mater. Sci.*, 2009, **44** , 5049 —5062 CrossRef CAS .
[4] K. S. Ramadan, D. Sameoto and S. Evoy, A review of piezoelectric polymers as functional materials for electromechanical transducers, *Smart Mater. Struct.*, 2014, **23** , 33001 CrossRef .
[5] S. B. Lang and S. Muensit , Review of some lesser-known applications of piezoelectric and pyroelectric polymers, *Appl. Phys. A: Mater. Sci. Process.*, 2006, **85** , 125 —134 CrossRef CAS .
[6] Maiti, S., Karan, S. K., Kim, J. K., & Khatua, B. B. (2019). Nature Driven Bio-Piezoelectric/Triboelectric Nanogenerator as Next-Generation Green Energy Harvester for Smart and Pollution Free Society. *Advanced Energy Materials*, *9*(9), 1803027.CrossRef .
[7] Narita, F., & Fox, M. (2018). A review on piezoelectric, magnetostrictive, and magnetoelectric materials and device technologies for energy harvesting applications. *Advanced Engineering Materials*, *20*(5), 1700743. CrossRef
[8] Chorsi, M. T., Curry, E. J., Chorsi, H. T., Das, R., Baroody, J., Purohit, & Nguyen, T. D. (2019). Piezoelectric biomaterials for sensors and actuators. *Advanced Materials*, *31*(1), 1802084. CrossRef
[9] D.-W. Fu *et al.*, Diisopropylammonium Bromide Is a High-Temperature Molecular Ferroelectric Crystal, *Science*, 2013, **339** , 425 —428 CrossRef CAS PubMed .
[10] S. Horiuchi *et al.*, Above-room-temperature ferroelectricity in a single-component molecular crystal, *Nature*, 2010, **463** , 789 —792 CrossRef CAS PubMed .
[11] David, C., Capsal, J. F., Laffont, L., Dantras, E., & Lacabanne, C. (2012). Piezoelectric properties of polyamide 11/NaNbO3 nanowire composites. Journal of Physics D: Applied Physics, 45(41), 415305. CrossRef
[12] W. Gao *et al.*, Flexible organic ferroelectric films with a large piezoelectric response, *NPG Asia Mater.*, 2015, **7** , e189 CrossRef CAS .
[13] Z. Zhang *et al.*, Tunable electroresistance and electro-optic effects of transparent molecular ferroelectrics, *Sci. Adv.*, 2017, **3** , e1701008 CrossRef PubMed .
[14] Katsouras *et al.*, The negative piezoelectric effect of the ferroelectric polymer poly(vinylidene fluoride), *Nat. Mater.*, 2016, **15** , 78 —84 CrossRef CAS PubMed
[15] Liu, Z. H., Pan, C. T., Lin, L. W., Huang, J. C., & Ou, Z. Y. (2013). Direct-write PVDF nonwoven fiber fabric energy harvesters via the hollow cylindrical near-field electrospinning process. Smart materials and structures, 23(2), 025003. CrossRef
[16] M. Owczarek *et al.*, Flexible ferroelectric organic crystals, *Nat. Commun.*, 2016, **7** , 13108 CrossRef CAS PubMed
[17] Khan, A., Abas, Z., Kim, H. S., & Oh, I. K. (2016). Piezoelectric thin films: an integrated review of transducers and energy harvesting. Smart Materials and Structures, 25(5), 053002. CrossRef
[18] S. Horiuchi , J. Tsutsumi , K. Kobayashi , R. Kumai and S. Ishibashi , Piezoelectricity of strongly polarized ferroelectrics in prototropic organic crystals, *J. Mater. Chem. C*, 2018, **6** , 4714 —4719 RSC.
[19] Ramadan, K. S., Sameoto, D., & Evoy, S. (2014). A review of piezoelectric polymers as functional materials for electromechanical transducers. Smart Materials and Structures, 23(3), 033001. CrossRef

[20] Levitskii, R. R., Zachek, I. R., Verkholyak, T. M. & Moina, A. P. Dielectric, piezoelectric, and elastic properties of the Rochelle salt NaKC 4 H 4 O 6· 4 H 2 O: A theory. *Physical Review B* **67**, 174112 (2003). CrossRef
[21] Solans, X., Gonzalez-Silgo, C., & Ruiz-Pérez, C. (1997). A structural study on the Rochelle salt. *Journal of solid state chemistry*, *131*(2), 350-357. CrossRef
[22] Valasek, J. (1922). Piezo-electric activity of Rochelle salt under various conditions. *Physical Review*, *19*(5), 478. CrossRef
[23] Lemaire, E., Moser, R., Borsa, C. J., & Briand, D. (2016). Green paper-based piezoelectronics for sensors and actuators. *Sensors and Actuators A: Physical*, *244*, 285-291. CrossRef
[24] Lemaire, E., Ayela, C., & Atli, A. (2018). Eco-friendly materials for large area piezoelectronics: self-oriented Rochelle salt in wood. *Smart Materials and Structures*, *27*(2), 025005. CrossRef
[25] Lemaire, E., Thuau, D., Souêtre, M., Zgainski, L., Royet, A., & Atli, A. (2021). Revisiting two piezoelectric salts within an eco-design paradigm for sensors and actuators applications. Sensors and Actuators A: Physical, 318, 112483. CrossRef
[26] Mason, W. P. (1947). Theory of the ferroelectric effect and clamped dielectric constant of rochelle salt. *Physical Review*, 72(9), 854. CrossRef
[27] Diamant, H., Drenck, K., & Pepinsky, R. (1957). Bridge for accurate measurement of ferroelectric hysteresis. Review of scientific instruments, 28(1), 30-33. CrossRef
[28] Wieder, H. H. (1958). Ferroelectric polarization reversal in rochelle salt. *Physical Review*, 110(1), 29. CrossRef